

CrystEngComm

Accepted Manuscript



This is an *Accepted Manuscript*, which has been through the Royal Society of Chemistry peer review process and has been accepted for publication.

Accepted Manuscripts are published online shortly after acceptance, before technical editing, formatting and proof reading. Using this free service, authors can make their results available to the community, in citable form, before we publish the edited article. We will replace this *Accepted Manuscript* with the edited and formatted *Advance Article* as soon as it is available.

You can find more information about *Accepted Manuscripts* in the [Information for Authors](#).

Please note that technical editing may introduce minor changes to the text and/or graphics, which may alter content. The journal's standard [Terms & Conditions](#) and the [Ethical guidelines](#) still apply. In no event shall the Royal Society of Chemistry be held responsible for any errors or omissions in this *Accepted Manuscript* or any consequences arising from the use of any information it contains.

Synthesis, structure, topology and magnetic properties of new coordination polymers based on 5(-Br/-COOH)-substituted nicotinic acid

Goutam Nandi,* Ranjit Thakuria, Hatem M. Titi, Ranjan Patra and Israel Goldberg*

School of Chemistry, Sackler Faculty of Exact Sciences, Tel-Aviv University, Ramat-Aviv, 69978 Tel-Aviv, Israel. E-mail: gtn.nd@gmail.com, goldberg@post.tau.ac.il

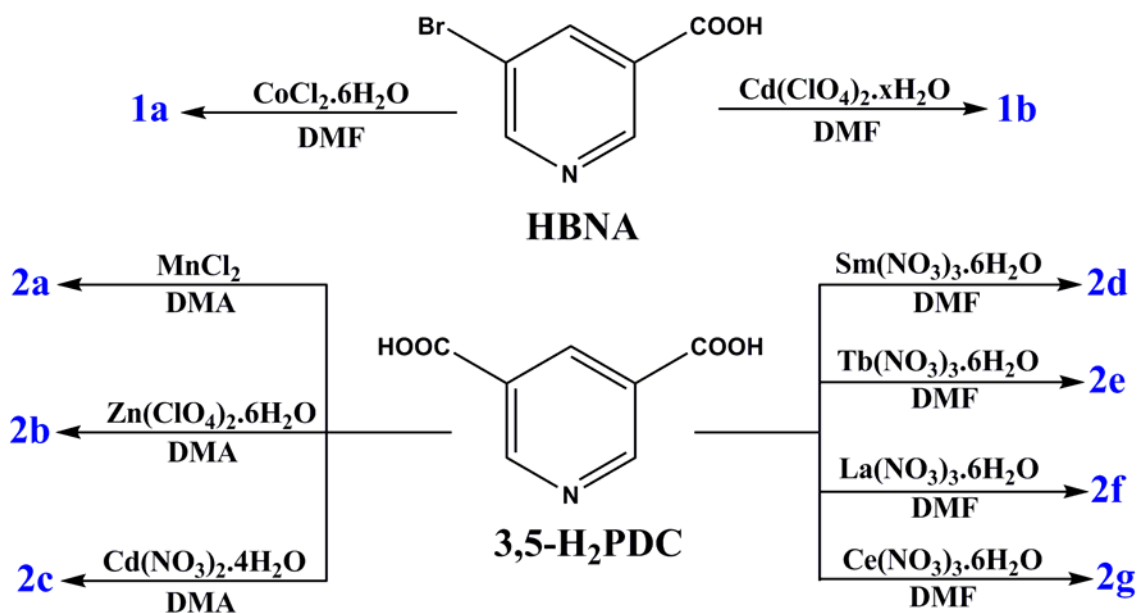
Abstract:

Nine new coordination polymers of 5-substituted nicotinic acid (with either -Br, HBNA, or -COOH, 3,5-H₂PDC) with d-transition (Co, Ni, Zn and Cd) and f-lanthanoid (La, Ce, Sm and Tb) metal ions have been synthesized. The two metal complexes [Co₂(BNA)₄(H₂O)]_n.H₂O (**1a**) and [Cd(BNA)₂]_n (**1b**) have polymorphic/isomeric structures to those of metal-organic-frameworks (MOFs) with similar structural building units (SBUs) reported earlier. Modified reaction conditions yielded new isomeric/pseudo-polymorphic metal complexes in the present case. Reactions of the 3,5-H₂PDC linker with different metal ions led to the formation of polymeric complexes [Mn₃(3,5-PDC)₃(DMA)₃]_n.DMA (**2a**), [Zn(3,5-PDC)(DMA)]_n.DMA (**2b**) and [Cd₂(3,5-PDC)₂(DMA)₄]_n (**2c**), as well as lanthanoid MOFs [Sm(3,5-PDC)_{1.5}(DMF)]_n.DMF (**2d**, as well as isomorphous products with La (**2f**) and Ce (**2g**) ions) and [Tb₂(3,5-PDC)₃(DMF)₂]_n.DMF (**2e**). Networking diversity observed in these coordination polymers with the conformationally rigid 5-substituted nicotinic acid ligand is discussed. The magnetic properties of **2a**, **2d** and **2e** have been studied as well.

Introduction

Metal-organic frameworks (MOF) have gained a huge interest during the last few decades not only because of their structural diversity, but also due to a large number of material applications.¹ A large number of MOFs utilizing rigid as well as flexible ligands and exhibiting various network topologies are reported in the literature. In recent past, our group has been also involved in the study of MOFs with flexible ligands, containing both the pyridyl and carboxylate donor arms.² As an extension of that project in this work we investigated formation of coordination polymers with smaller but more rigid organic linkers as 5-bromonicotinic acid (HBNA) and 5-carboxynicotinic acid (3,5-pyridinedicarboxylic;

H₂PDC). Various polymeric assemblies involving bromonicotinate (BNA) have been documented in the literature.³ The present choice of this building unit has been made to explore the possibility of the bromine substituent to be involved in extra halogen bonding interactions in the formed networks, an issue not discussed in the previously reported structures. The tri-dentate 3,5-H₂PDC ligand can readily coordinate to the d-block as well as f-block metal ions due to the presence of two carboxylic donor arms and one pyridyl arm to promote the formation of framework architectures. Despite the commercial availability of H₂PDC very few MOF structures of this ligand have been reported in the literature so far.⁴ Most recently, while our work was already in progress, the luminescent properties of some 3,5-PDC lanthanoid coordination polymeric complexes bearing glycolate or acetate as ancillary ligand have been published.⁵ This article deals with the synthesis, structure, topology and magnetic properties of seven new coordination polymers (**1a-2e**) with BNA and 3,5-PDC as linkers and various metal ion connectors (Scheme 1). Reactions of 3,5-H₂PDC with La and Ce ions yielded MOFs **2f** and **2g** (respectively) which are isomorphous with that of **2d**. They reveal however unique formation of metallogels when reacted with other solvents, the properties of which will be discussed in more detail in a separate publication.⁶



Scheme 1. Coordination complexes of HBNA and 3,5-H₂PDC ligands with d-transition and f-lanthanoid metal salts analyzed in this study.

Experimental Section:

Materials and Methods: All the reagents are commercially available and were used without further purification. The FT-IR spectra were recorded on a Bruker Tensor 27 system spectrophotometer in ATR mode. The magnetic data were collected on a Quantum Design MPMS SQUID-XL-5 magnetometer using crushed single-crystal samples. Magnetic data were corrected for the diamagnetic contribution calculated from Pascal constants⁷ and a background of the sample holder. Complexes **1a-2e** were prepared by solvothermal reactions as described below.

Synthesis of 1a: CoCl₂·6H₂O (10 mg, ~0.04 mmol), and HBNA (5 mg, ~0.025 mmol) are taken in a screw capped glass sample vial (4 mL) containing 3 mL dimethylformamide (DMF). The mixture is sonicated well to obtain a clear solution and then heated at 120 °C in a bath-reactor for 24 hours. On cooling to room temperature, magenta colored crystals of complex **1a** were obtained. Yield: 62 %. Anal. Calcd. For C₂₄H₁₅O₁₀N₄Br₄Co₂: C, 30.12; H, 1.58; N, 5.86. Found: C, 31.21; H, 1.61; N, 5.65. FT-IR (cm⁻¹): 1621 (s, b, ν_{C=O} asymmetric), 1471 (s, ν_{C=C}), 1285 (m, ν_{C=O} symmetric), 1187 (s, ν_{C-O}), 1123, 1087, 857, 729, 681.

Synthesis of 1b: This complex was prepared by following similar methodology as described for **1a** using Cd(ClO₄)₂·xH₂O instead of CoCl₂·6H₂O. Yield: 56 %. Anal. Calcd. For C₁₂H₆O₄N₂Br₂Co: C, 28.02; H, 1.18; N, 5.45. Found: C, 28.11; H, 1.23; N, 5.56. FT-IR (cm⁻¹): 1605 (s, ν_{C=O} asymmetric), 1497 (s, ν_{C=C}), 1296 (m, ν_{C=O} symmetric), 1189 (s, ν_{C-O}), 1104, 1064, 879, 749, 687.

Synthesis of 2a: A mixture of H₂PDC (5 mg, 0.03 mmol) and anhydrous MnCl₂ (3.8 mg, ~0.03 mmol) are taken in a screw capped glass sample vial (4 mL) containing 2.5 mL dimethylacetamide (DMA). Two drops of conc. HNO₃ is added to it and sonicated well to get a clear solution. The solution is then heated at 120 °C for 24 hours in a bath-reactor. Needle shaped colorless crystals of **2a** were obtained on cooling to room temperature. Crystals were separated by filtration and washed with DMA, dried in air. Yield: 63 %. Anal. Calcd. For C₃₅H₃₉O₁₅N₇Mn₃: C, 43.67; H, 4.08; N, 10.18. Found: C, 44.21; H, 4.31; N, 10.88. FT-IR (cm⁻¹): 1600 (s, ν_{C=O} asymmetric), 1502 (s, ν_{C=C}), 1298 (m, ν_{C=O} symmetric), 1206 (s, ν_{C-O}), 1148, 1030, 847, 749, 693.

Synthesis of 2b: A mixture of H₂PDC (5 mg, 0.03 mmol) and Zn(ClO₄)₂·6H₂O (11 mg, ~0.03 mmol) are taken in a screw capped glass sample vial (4 mL) containing 2.5 mL DMA. 2-3 minutes of sonication gave a clear solution. The solution is then heated at 120 °C for 24 hours in a bath-reactor. Block shaped colorless crystals of **2b** were obtained on cooling to room temperature. Crystals were separated by filtration and washed with DMA, dried in air. Yield: 68 %. Anal. Calcd. For C₁₅H₂₁O₆N₃Zn: C, 44.51; H,

5.23; N, 10.38. Found: C, 44.96; H, 5.62; N, 10.68. FT-IR (cm^{-1}): 1603 (s, $\nu_{\text{C=O}}$ asymmetric), 1502 (s, $\nu_{\text{C=C}}$), 1344(m, $\nu_{\text{C=O}}$ symmetric), 1283 (s, $\nu_{\text{C-O}}$), 1130, 1032, 828, 767, 737.

Synthesis of 2c: This polymer was prepared by similar methodology as described for **2a** using $\text{Cd}(\text{NO}_3)_2 \cdot 4\text{H}_2\text{O}$ instead of MnCl_2 . Yield: 63 %. Anal. Calcd. For $\text{C}_{15}\text{H}_{21}\text{O}_6\text{N}_3\text{Cd}$: C, 39.88; H, 4.69; N, 9.3. Found: C, 41.11; H, 4.91; N, 10.28. FT-IR (cm^{-1}): 1599 (s, $\nu_{\text{C=O}}$ asymmetric), 1502 (s, $\nu_{\text{C=C}}$), 1281 (m, $\nu_{\text{C=O}}$ symmetric), 1260 (s, $\nu_{\text{C-O}}$), 1126, 1021, 834, 773, 740.

Syntheses of 2d and 2e: A mixture of H_2PDC (5 mg, ~ 0.03 mmol) and $\text{Ln}(\text{NO}_3)_3 \cdot 6\text{H}_2\text{O}$ (Ln = Sm, Tb) in 1:1 stoichiometric amount were taken in a screw capped glass sample vial (4 mL) containing 2.5 mL DMF. The mixture was sonicated well to get a clear solution. The solution is then heated at 120 °C for 24 hours in a bath-reactor. Needle shaped colorless crystals of **2d** and **2e** were obtained on cooling to room temperature. Crystals were separated by filtration and washed with DMA, dried in air. Yield: 56 % and 55 % respectively. Data for **2d**: Anal. Calcd. For $\text{C}_{30}\text{H}_{30}\text{O}_{14}\text{N}_6\text{Sm}_2$: C, 36.06; H, 3.03; N, 8.41. Found: C, 37.13; H, 3.95; N, 8.52. FT-IR (cm^{-1}): 1597 (s, $\nu_{\text{C=O}}$ asymmetric), 1502 (s, $\nu_{\text{C=C}}$), 1290 (m, $\nu_{\text{C=O}}$ symmetric), 1250 (s, $\nu_{\text{C-O}}$), 1142, 1029, 830, 768, 721. Data for **2e**: Anal. Calcd. For $\text{C}_{30}\text{H}_{30}\text{O}_{14}\text{N}_6\text{Tb}_2$: C, 35.45; H, 2.97; N, 8.27. Found: C, 36.61; H, 3.42; N, 8.71. FT-IR (cm^{-1}): 1597 (s, $\nu_{\text{C=O}}$ asymmetric), 1501 (s, $\nu_{\text{C=C}}$), 1289 (m, $\nu_{\text{C=O}}$ symmetric), 1249 (s, $\nu_{\text{C-O}}$), 1144, 1030, 831, 767, 713. Additional reactions in similar experimental conditions with $\text{La}(\text{NO}_3)_3 \cdot 6\text{H}_2\text{O}$ and $\text{Ce}(\text{NO}_3)_3 \cdot 6\text{H}_2\text{O}$ yielded solid products (**2f** and **2g**, respectively) with are isomorphous to **2d**,

X-ray Crystallographic Determination. Single crystal data for the complexes **1a**, **1b** and **2a-2g** were collected at 110(2) K, using a Bruker's Apex-Duo diffractometer with $\text{Mo K}\alpha$ ($\lambda = 0.71075 \text{ \AA}$) radiation. Crystal structures were solved by direct methods and refined by full-matrix least squares (SIR-97, SHELXS and SHELXL-97).^{8,9} The crystallographic and experimental data are given in Table 1. The uniform bulk properties of the analyzed materials were confirmed by elemental analysis (see above). CCDC 981479-981485 (**1a-2e**), 979166 (**2f**) and 979167 (**2g**).

Results and Discussion

Structure and topology

HBNA is a bidentate ligand with one pyridyl-N and one carboxylic acid coordinating arms. Whereas, 3,5- H_2PDC is a tridentate ligand with one pyridyl-N and two carboxylic acid coordinating arms. Seven new coordination polymeric complexes (**1a-2e**) have been synthesized and fully characterized by single crystal X-ray diffraction analysis using these two ligands. Complexes **1a** and **1b** show completely different structural behavior with respect to the previously reported MOFs, even though they possess similar

structural building units (SBUs).¹⁰ Correspondingly, complexes **1a** and **1b** can be referred to as pseudo-polymorphs/supramolecular isomers of the already published structures. Descriptions of the crystal structures can be simplified by using the node-and-linker approach in the TOPOS (v. 4.0) software.¹¹ In the network structures shown below in the various Figures, the metal and linker moieties are marked by blue and red color respectively.

Crystal Structure of 1a: With respect to the known anhydrous $[\text{Co}(\text{BNA})_2(\text{H}_2\text{O})]$ MOF (solved in monoclinic $C2/c$),¹⁰ complex **1a** crystallizes in monoclinic $P2_1/n$ space group with two Co(II) ions, four BNA ligands, one coordinated water and one disordered free solvent water molecule. The two MOFs have exactly the same structural building unit (SBU) (Figure 1a) with aquadicarboxylate triply-bridged Co(II) dimer connected by bidentate- and tridentate-bridging BNA with coordination mode $\mu_2\text{-}\kappa\text{O}:\kappa\text{N}$ (Scheme 2a) and $\mu_3\text{-}\kappa\text{O}:\kappa\text{O}:\kappa\text{N}$ (Scheme 2b) respectively. The Co...Co distance within the dinuclear cluster is 3.543 Å which is slightly longer than the reported anhydrous MOF (3.512 Å), and Co-O_w-Co angle is 114.13°. The Co(II) ions exhibit distorted CoN₂O₄ octahedral coordination geometry (angles around the metal ion are within the range of 82.37(1)–94.20(1)°) generated by two pyridine N, three carboxylate O and one bridging water molecule. The dinuclear Co₂ unit is surrounded by six Co(II) ion to form a 3D framework structure having channels along {001} axis, the bromo groups oriented towards the channels are offset to each other with Br...O halogen bonding interaction of 3.032 Å (the sum of the corresponding van der Waals radii is 3.35 Å)¹². The channels are occupied by disordered solvent water molecules (Figure 1b). The disordered solvent water molecule could not be modeled, hence removed using SQUEEZE command. Due to the extra water solvent content MOF **1a** can be considered as a pseudo-polymorph of the reported Co-MOF. By considering the dinuclear Co₂ cluster as a node and BNA ligand as a linker (Figure 1c) it gives (2,8) connected 2-nodal net with Schlafli symbol $\{4^4.12^{24}\}\{4\}_4$ (Figure 1d).

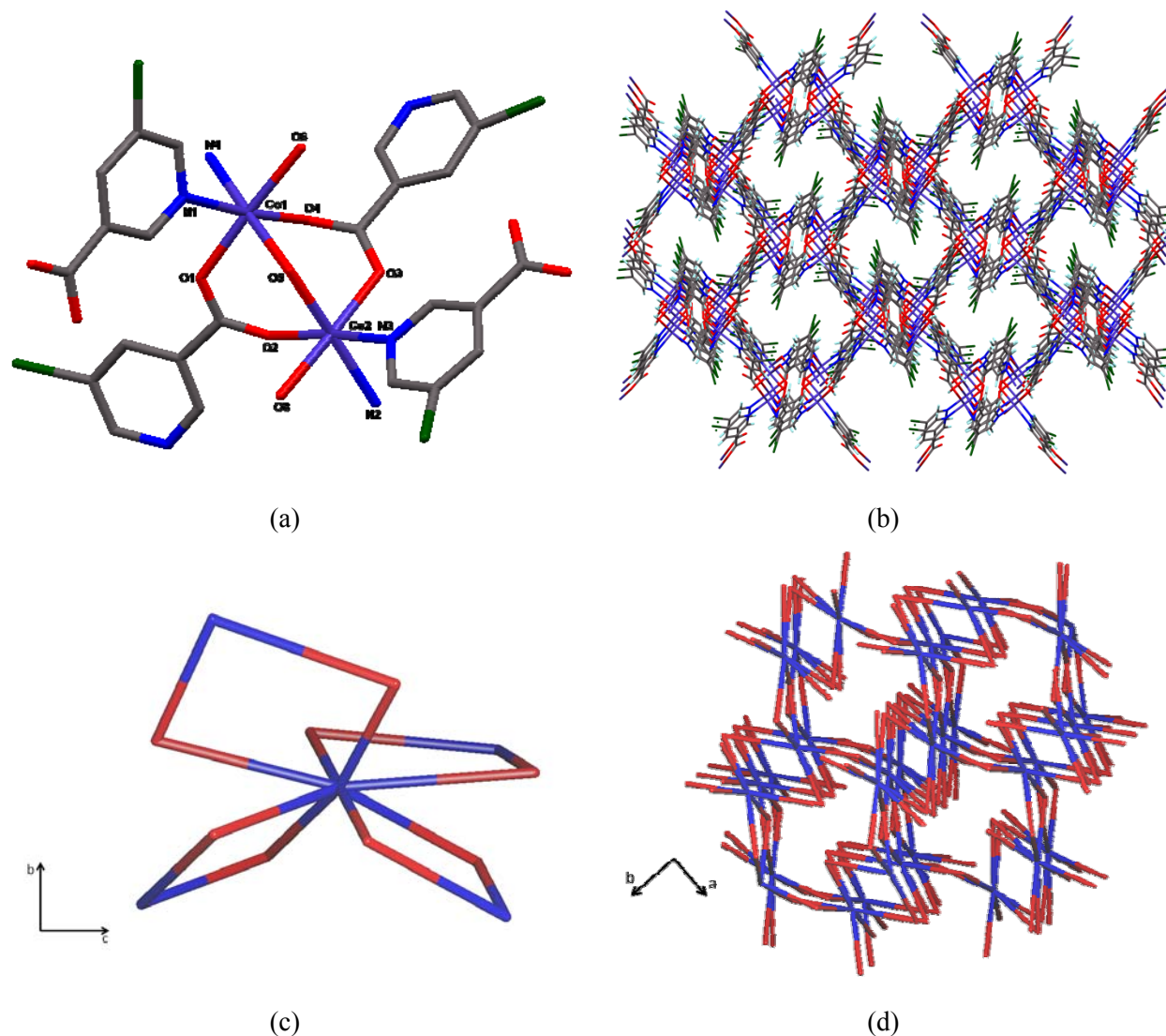
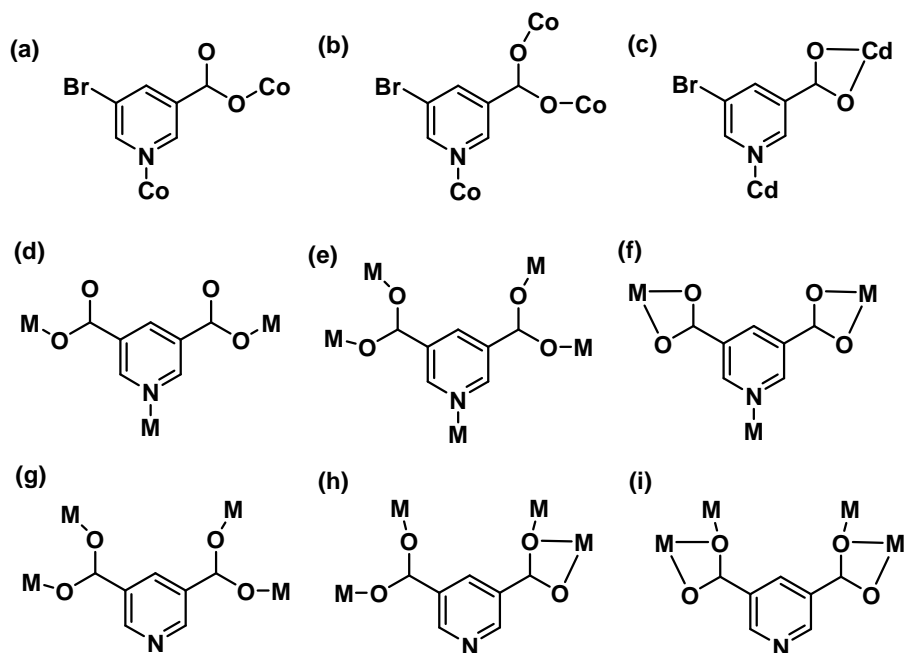


Figure 1. (a) View of the SBU of complex **1a** with the Co-centers denoted in blue color (hydrogen atoms are omitted for clarity). (b) 3D packing of **1a** view along ab plane. (c) Coordination environment across dinuclear metal cluster node. (d) The topology of **1a** framework.

Crystal Structure of 1b: The complex has the same stoichiometry as that of the reported MOF.¹⁰ The crystal structure of **1b** reveals the $C2/c$ space-group symmetry. The two structures have similar SBU and connectivity (Figure 2a). The central metal Cd(II) is having a distorted octahedral coordination environment (bond angles around the metal are within the range of $82.41(8)$ – $111.46(7)^\circ$), generated by two pyridyl-N atoms and four carboxylate O atoms belonging to two BNAs with coordination mode μ_2 - $\kappa O_2O:\kappa N$ (Scheme 2c). Thus, the central metal atom is surrounded by four Cd(II) metal ions. The SBU of formerly published structure has two N atoms at *trans* position, whereas in complex **1b** the two N atoms

are having *cis* related geometry, as a result they have different structural arrangement (Figure 2b). The reported structure represents a 3D framework,¹⁰ while complex **1b** shows a 2D framework with strong Br...O halogen bonding interaction ($d = 2.934 \text{ \AA}$, which is shorter by about 0.3 \AA from the corresponding van der Waals distance)¹² (Figure 2c). The topology of the resulting structure can be defined as (2,4) connected 2-nodal net with the Schläfli symbol $\{8^4.12^2\}\{8\}_2$ (Figure 2d). Therefore we can consider these two structures as supramolecular isomers, a phenomenon frequently observed for coordination polymers¹³ as opposed to simple polymorphism.¹⁴



Scheme 2 Coordination environments of the BNA and 3,5-PDC ligands exhibited in the present study.

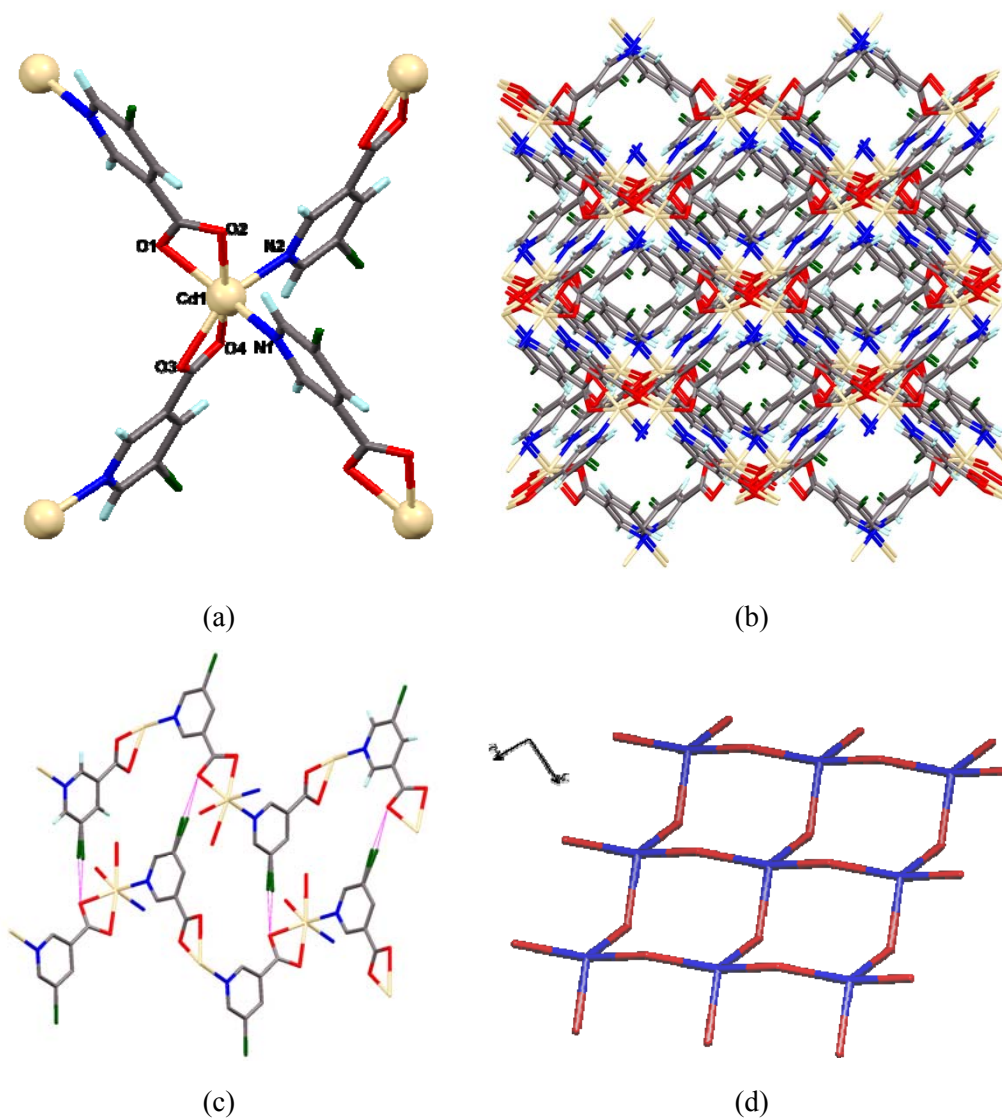


Figure 2. (a) SBU of **1b**. (b) 3D packing of **1b** view along *ab* plane. (c) 2D framework with strong Br \cdots O interaction (pink dotted line). (d) The topology of **1b** framework.

Crystal Structure of 2a: Complex **2a** crystallizes in monoclinic $P2_1/n$ space group. The asymmetric unit consists of three Mn(II) ion, three 3,5-PDC ligands, three coordinated and one (disordered) free solvent DMA molecules. All three Mn(II) ions are in a distorted octahedral coordination geometry (angles within the range of $80.80(1)$ – $101.50(1)^\circ$) having a trinuclear hourglass SBU (Figure 3a) with Mn–O distance ranges from $2.095(4)$ to $2.341(3)$ Å; Mn–N of $2.347(4)$ Å (Mn2–N17) and $2.266(4)$ Å (Mn3–N16). Mn2 is surrounded by [NO₅] donor set, generated by three carboxylate oxygens (O4, O13 and O14) of three 3,5-PDC units, one nitrogen atom (N17) from one 3,5-PDC moiety and two coordinated DMA solvents (O46 and O51) respectively. The central metal atom Mn1 is surrounded by six carboxylate oxygens (O6, O7, O8, O9, O11 and O12) from three different 3,5-PDC ligands. The terminal Mn3 ion is coordinated to

four carboxylate oxygens (O5, O6, O10 and O15) from three different 3,5-PDCs, one nitrogen atom (N16) from one 3,5-PDC and a coordinated solvent DMA (O40). The three 3,5-PDC have different coordination mode, two of them having $\mu_5\text{-}\kappa\text{O}:\kappa\text{O}:\kappa\text{O}:\kappa\text{O}:\kappa\text{N}$ (Scheme 2e) and one with $\mu_4\text{-}\kappa\text{O}:\kappa\text{O}:\kappa\text{O}:\kappa\text{O},\text{O}$ (Scheme 2h). Complex **2a** forms a 3D framework characterized as (2,3,8) connected 3-nodal net with Schläfli symbol $\{4^3\}_2\{4^7.6^6.8^{11}.10^4\}\{4\}$ (Figure 3b-c). The disordered free DMA solvent occupies the channels created by the network structure along the b-axis.

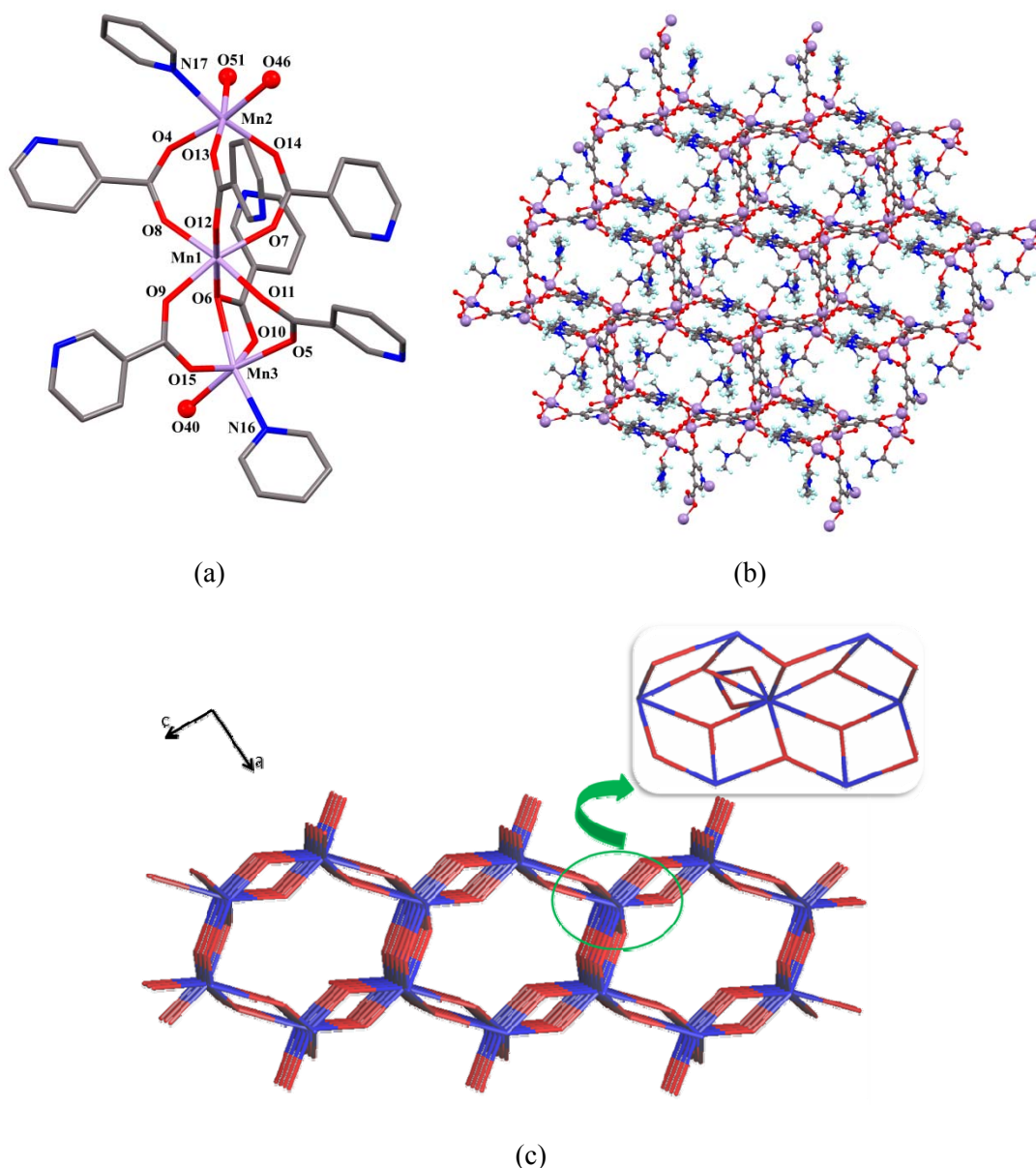
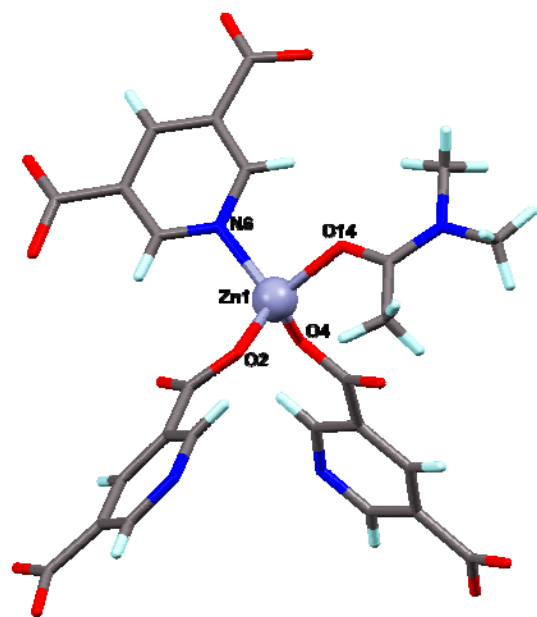
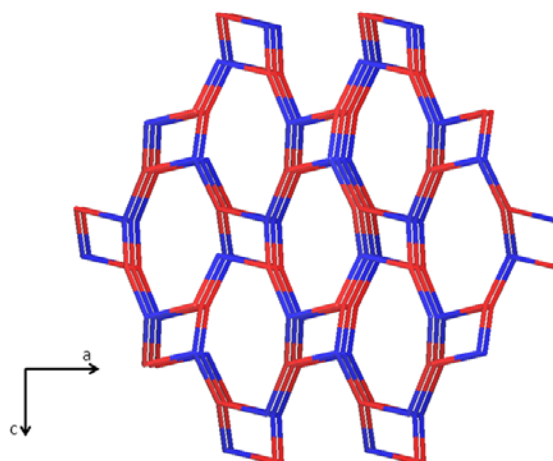


Figure 3. (a) Trinuclear hourglass SBU of **2a** (red spheres in represent coordinated DMA molecules; hydrogen atoms are omitted for clarity). (b) 3D framework packing viewed along *ac* plane with coordinated solvent DMA pointing towards the channels occupied by disordered non-coordinated DMA molecules. (c) The topology of complex **2a**.

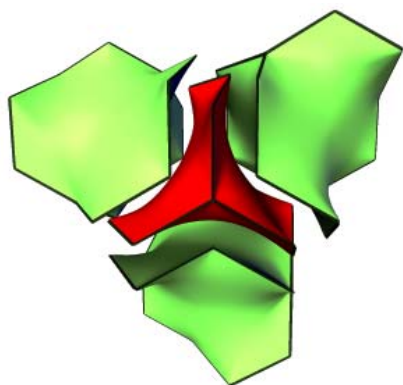
Crystal Structure of 2b: The complex crystallizes in orthorhombic $P2_12_12_1$ space group. The asymmetric unit consist of one Zn(II) ion, one 3,5-PDC ligand, one coordinated and one disordered free solvent DMA molecules. The Zn(II) ion is having a tetrahedral geometry surrounded by $[\text{NO}_3]$ donor set, generated by two carboxylate O atoms of two 3,5-PDC ligands, one O atom from the coordinated solvent DMA and one N atom of 3,5-PDC (Figure 4a). The Zn–O length varies from 1.936(2) to 1.971(2) Å, and Zn–N with a distance of 2.039(2) Å (Zn1–N6). 3,5-PDC acts as tridentate ligand with $\mu_3\text{-}\kappa\text{O}:\kappa\text{O}:\kappa\text{N}$ coordination mode (Scheme 2d). As one of the coordinating sites is blocked by solvent DMA molecule, both the metal Zn(II) and ligand 3,5-PDC act as three-connector nodes, resulting a 3D chiral **srs** type network with Schläfli symbol $\{10^3\}$ (Figure 4b). The tiling pattern of the **srs** net can be shown (Figure 4c) with a representation $[10^3]$, using Systre and 3dt.¹⁵ The tiling has a point symmetry no. 32 with 8 nodes and 12 edges for each repeated unit (Figure 4d). The **srs** net contains rectangular channels along the $\{100\}$ axis filled with disordered solvent DMA molecules (Figure 4e). Due to the solvent inclusion, no interpenetration is possible in this particular framework. Packing fraction and total potential solvent area volume were calculated using PLATON after removing the included DMA solvent. The packing index value of 50.6 % and solvent area volume of 646.8 Å³, showed the complex to be potentially porous with wide solvent-accessible channels (Figure 4f).



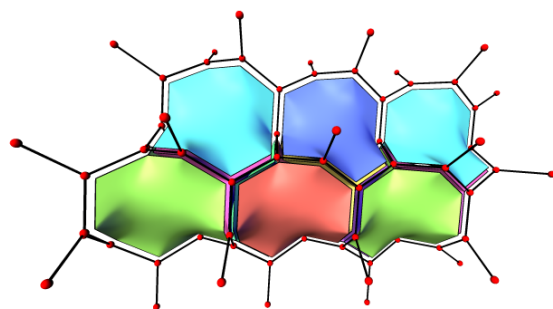
(a)



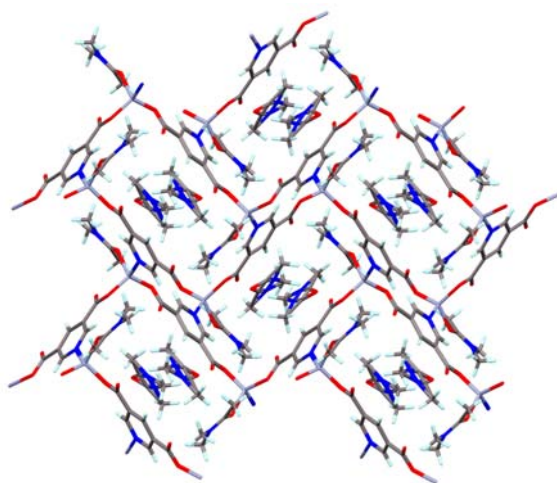
(b)



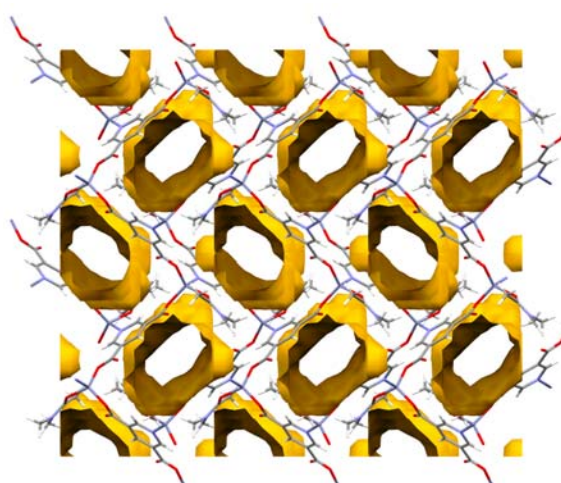
(c)



(d)



(e)



(f)

Figure 4. (a) Tetrahedral SBU of **2b**. (b) Topological **srs** network formed by complex **2b**. (c) Natural tiling of **2b**.¹⁵ (d) The tiling with net of vertices and edges. (e) 3D framework packing with disordered solvent DMA occupying the channels along {100} axis. (f) Network channels are modeled using the program Mercury with void volume of 538.89 Å³ (30 % of unit cell volume).

Crystal Structure of 2c: The complex **2c** crystallizes in a monoclinic $P2_1$ chiral space group with the asymmetric unit consisting of two Cd(II) ions, two 3,5-PDCs and four coordinated solvent DMA molecules. The Cd(II) ions are seven coordinated by four carboxylate O atoms of two 3,5-PDCs, one N atom of one 3,5-PDC and two DMA molecules forming a pentagonal bipyramidal geometry with [NO₆] donor mode (Figure 5a). The Cd–O distance varies from 2.270(3) to 2.663(3) Å; Cd–N distances are 2.309(4) Å (Cd1–N11) and 2.318(3) Å (Cd2–N12). Both the 3,5-PDCs are tridentate and adopt μ_3 - $\kappa O,O:\kappa O,O:\kappa N$ coordination mode (Scheme 2f). Two DMA molecules coordinate to the metal along the *trans*-related axial positions. As a result **2c** forms a 2D framework structure having 3 connected uninodal net of topological type **hcb** with Schläfli symbol {6³} (Figure 5b-c). The metal connected infinite 2D grids are stacked parallel to each other along (101) plane, and the vacant space created by the layers is occupied by dangling solvent DMA molecules as shown in Figure 5b.

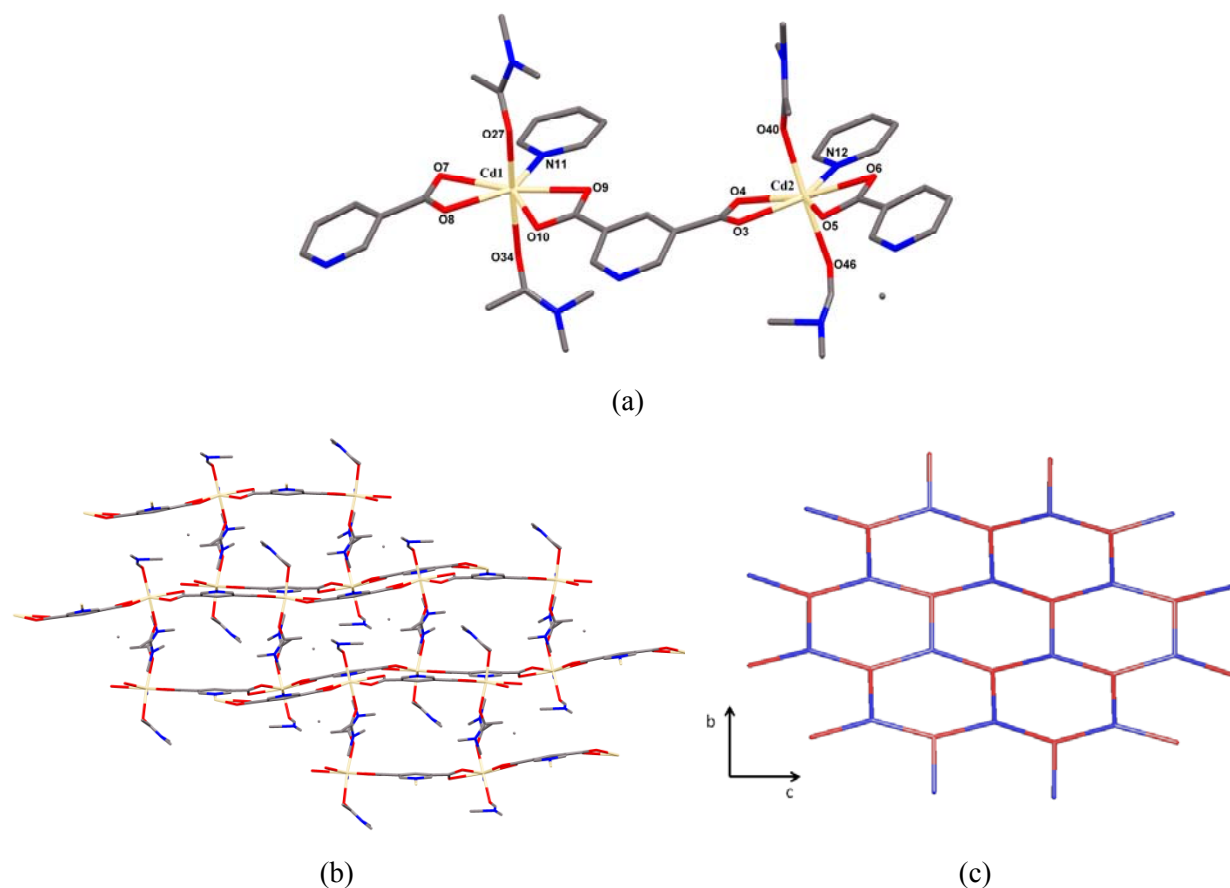


Figure 5. (a) Trigonal bipyramidal SBU of **2c** (hydrogen atoms are omitted for clarity). (b) 2D framework stacked parallel to each other along (101) plane with dangling solvent molecules. (c) The topological **hcb** network formed by **2c**.

Crystal structures of [Ln(III)(3,5-PDC)_{1.5}(DMF)]_xDMF (Ln = Sm (2d**), La (**2f**), Ce (**2g**):** Framework structures **2d**, **2f** and **2g** crystallize in orthorhombic *Pnma* space group and are isomorphous, structure **2d** being discussed below. In **2d**, the asymmetric unit consists of one symmetry independent Sm(III) ion, one and half molecules of 3,5-PDC, one coordinated and one disordered free solvent (removed using SQUEEZE command) DMF molecules. The nine coordinated Sm(III) ion has a distorted mono-capped square antiprism geometry (angles around Sm are within the range of 70.06(8)–147.46(9)°) (Figure 6a). The [O₉] donor set of Sm(III) ion is generated by eight carboxylate oxygen atoms of six 3,5-PDCs and one coordinated solvent DMF molecule. Unlike in the d-metal complexes, only the carboxylate O atoms take part in metal coordination due to the prominent oxophilic nature of the lanthanoid ions. The pyridyl-N site of the ligand remains free to interact with the solvent species. The 3,5-PDC ligand adopts two different coordination modes $\mu_4\text{-}\kappa\text{O}:\kappa\text{O}:\kappa\text{O}:\kappa\text{O},\text{O}$ (Scheme 2h) and $\mu_4\text{-}\kappa\text{O}:\kappa\text{O},\text{O}:\kappa\text{O}:\kappa\text{O},\text{O}$ (Scheme 2i) respectively. The Sm(III) ions are connected to each other through carboxylate O, with Sm–O distances within 2.318(2)–2.740(2) Å forming a 1D polymeric chain (Figure 6b) with Sm⋯Sm separation distance of 4.249 Å. These polymeric 1D chains are inter-connected by bridging 3,5-PDC, giving rise to a (2,5) connected 2-nodal 3D net characterized by Schläfli symbol of $\{6^6.8.10^3\}_2\{6\}_3$ (Figure 6c), where each metal atom is considered as a node. The resulting network forms wide hexagonal solvent-accessible channels along {100} axis filled with disordered solvent DMF molecules (Figure 6d). The network structure exhibits tiling of a repeated unit with 20 nodes and 32 edges and can be represented as $[6^6.12^2]$. The dualized natural tiling¹⁵ possesses two nonequivalent tiles $2[3^2.4^3]$ and $3[4^2]$ with a **hex** net as shown in Figure 6e-f (in pink and green respectively).

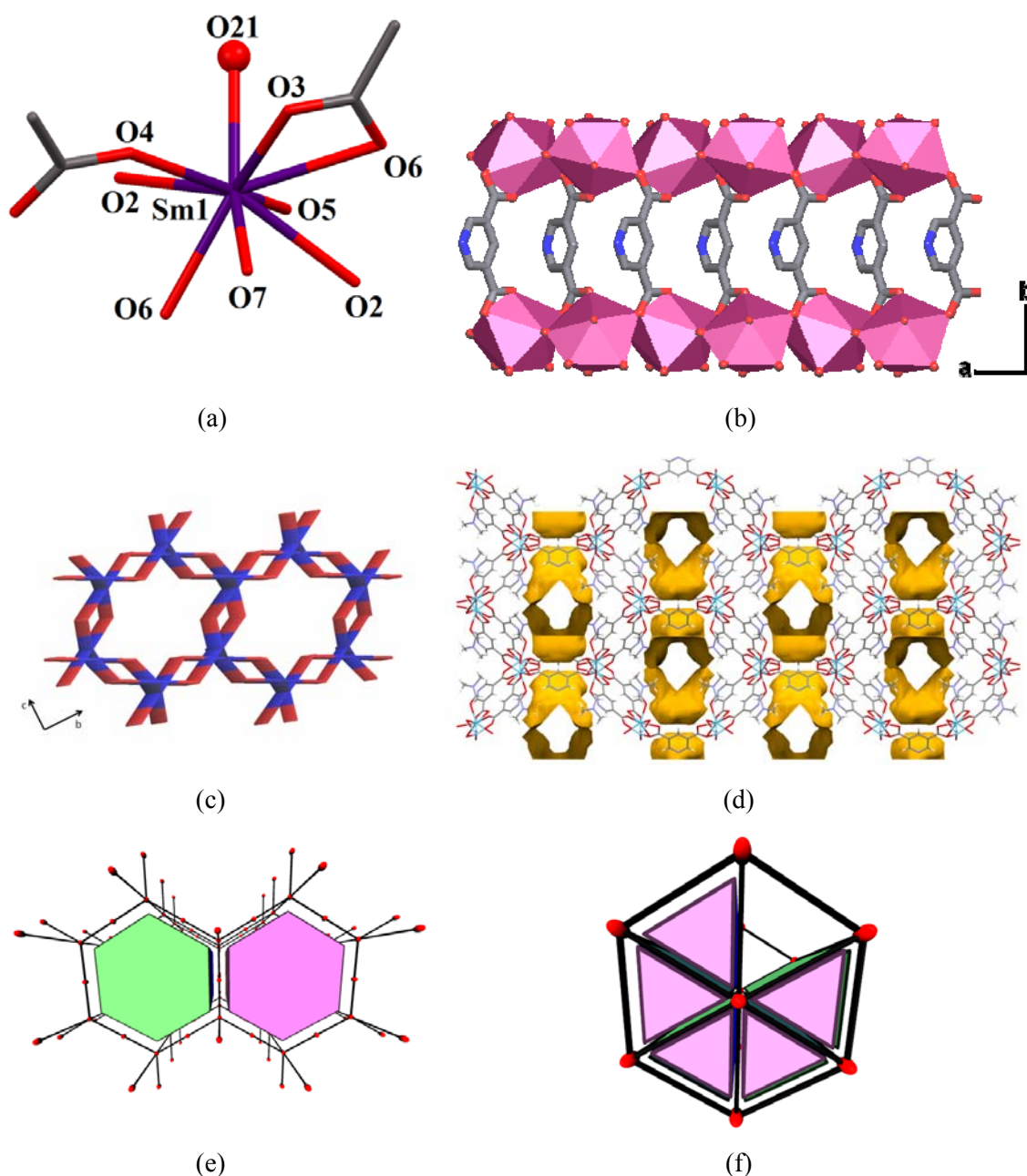
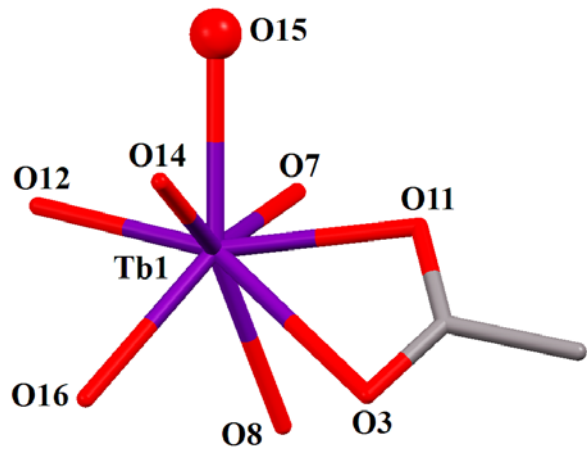


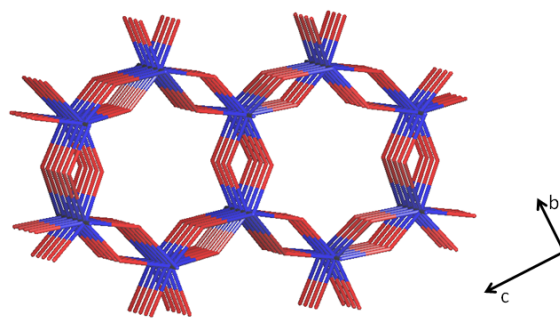
Figure 6. (a) View of the basic coordination environment of **2d**. (b) 1D polymeric chain formed by metal-oxygen bond along {100} axis. (c) The network topology of **2d** structure. (d) Network channels are modeled using the program Mercury with void volume of 647.45 Å³ and 17.4 % of unit cell volume. (e) Natural tiling of **2d**.¹⁵ (f) The dualized tiling of natural tile.¹⁵

Crystal structure of 2e: It crystallizes in space group $P2_12_12_1$ with cell parameters considerably different from those of the other lanthanoid MOFs (**2d**, **2f** and **2g**). The asymmetric unit consists of two Tb(III) ions, three 3,5-PDCs, two coordinated and one disordered free solvent DMF molecules. The Tb(III) ions

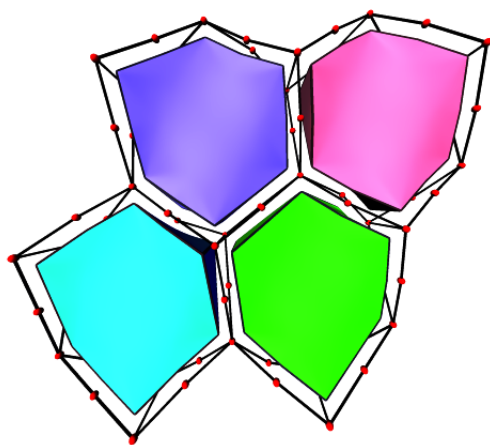
are eight-coordinate, each to seven carboxylate oxygen atoms of six 3,5-PDCs and one DMF molecule, to show a $[O_8]$ distorted square antiprism coordination geometry (Figure 7a). The three symmetry independent 3,5-PDCs adopt two different coordination modes $\mu_4\text{-}\kappa\text{O}:\kappa\text{O}:\kappa\text{O}:\kappa\text{O}$ (Scheme 2g) and $\mu_4\text{-}\kappa\text{O}:\kappa\text{O},\text{O}:\kappa\text{O}:\kappa\text{O},\text{O}$ (Scheme 2i). The pyridyl-N is not coordinated. Similar to the other lanthanoid MOFs, **2e** also contains oxo-bridged 1D polymeric chains having Tb–O distances in the range of 2.293(8)–2.847(9) Å with alternate Tb⋯Tb separation distance of 4.551 Å and 4.566 Å. By considering the two Tb–O connected clusters as a node and 3,5-PDC as a linker, crystal structure **2e** can be best represented as (2,8) connected 2-nodal net, having a Schläfli symbol of $\{5^9.6^6.7.8^6.9^6\}\{5\}_3$ (Figure 7b). The resulted network contains hexagonal channels along $\{100\}$ axis filled with disordered solvent DMF molecules similar to the other lanthanoid MOFs. The framework exhibits only one natural (Figure 7c) tiling represented as $[5^6.12^2]$ with total 16 nodes and 28 edges in the repeated unit. The network shows high symmetry dualized natural tiling (Figure 7d) with **hex** net having two kinds of tiles $[3^2.4^6]$ and $3[4^2]$. The basic difference between structure **2e** and **2d** is the coordination geometry across the metal ion ($[O_8]$ in **2e**, as opposed to $[O_9]$ in **2d**) and the topology of the 1D polymeric chains. The latter is (2,8)-connected in **2e** (Figure 7e) and (2,5)-connected in **2d** (Figure 7f).



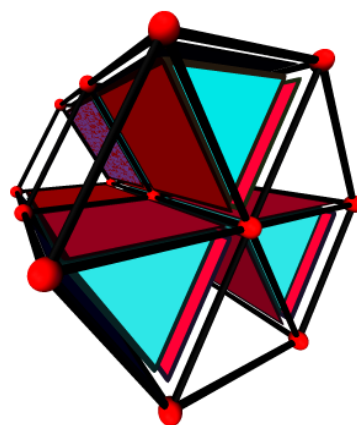
(a)



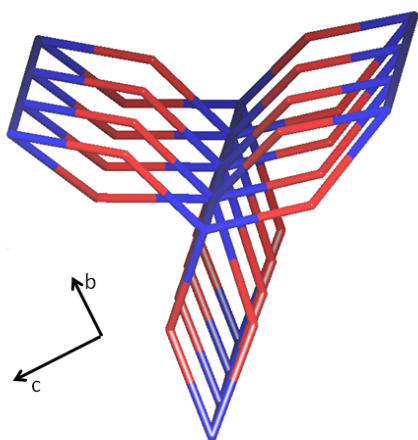
(b)



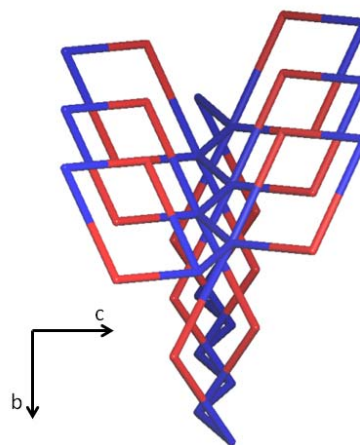
(c)



(d)



(e)



(f)

Figure 7. (a) View of the basic coordination environment of **2e** (O15 represents the coordinated DMF species). (b) The network topology of **2e** structure. (c) Natural tiling of **2e**.¹⁵ (d) The dualized tiling of natural tile.¹⁵ (e) 1D polymeric chain of **2e** with (2,8) connection. (f) 1D polymeric chain of **2d** with (2,5) topological connection.

Magnetic properties

Variable-temperature magnetic susceptibility measurements were performed on microcrystalline samples of compounds **2a**, **2d** and **2e**. The magnetic susceptibilities of the compounds were measured in the temperature range of 2–300 K under a 500 Oe field. The plots of $\chi_M T$ and χ_M vs. temperature of compound **2a** are shown in Figure 8. The experimental $\chi_M T$ value at 300 K is about 12.19 emu mol⁻¹K, is very close to calculated value 13.12 emu mol⁻¹K for three uncoupled Mn(II) ions with spin value 5/2 and Landé *g* value of 2.20.¹⁶ The $\chi_M T$ vs. temperature plot decreases slowly as the temperature decreases, at temperatures below 50 K the decrease in the $\chi_M T$ product is more pronounced. Upon cooling down to 2 K the value is 5.32 emu mol⁻¹K. The inverse susceptibility plot as a function of temperature is linear above 30 K, following the Curie–Weiss law with a Weiss constant, $\theta = -15.5$ K. The small negative Weiss constant suggests that there exists an antiferromagnetic interaction between two Mn(II) centers. The negative intercept for reciprocal susceptibility and the decreasing $\chi_M T$ value upon cooling indicates a slight antiferromagnetic interaction between the adjacent metal ions through carboxylate bridges which is also observed in related context.^{2,17}

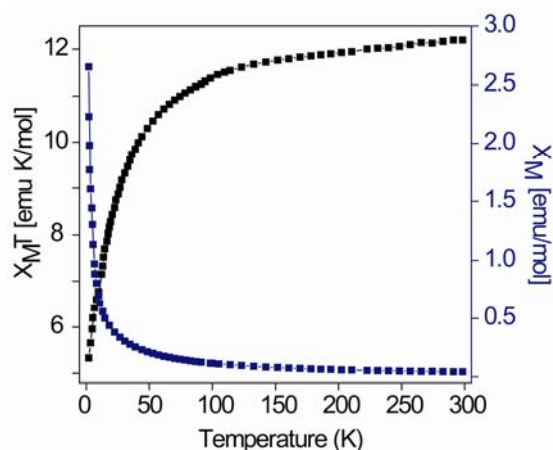


Figure 8. Plots of the temperature dependence of $\chi_M T$ and χ_M for compound **2a**.

The magnetic behaviors of **2d** and **2e** are different from **2a** due to the much weaker effects of the magnetic exchange coupling, as the *f* orbitals are well shielded by outer *s* and *p* orbitals and less extended compared to *d* orbitals of the Mn(II) ion. The spin–orbit coupling plays an important role in the magnetism of lanthanoids.¹⁶ Due to the influence of the inter-electronic repulsion and spin–orbit coupling, the 4*f*^{*n*} configuration of a Ln(III) ions split into ^{2*S*+1}L_{*J*} spectroscopic levels. Each of the states is further

split into Stark sublevels by the crystal field. The site symmetry of the Ln(III) ions determines the number of possible Stark sublevels. At ambient temperature, all Stark sublevels of the $^{2S+1}L_J$ ground state are thermally populated.¹⁶ As the temperature decreases, depopulation of these sublevels occurs and therefore $\chi_M T$ decreases. The variation of χ_M and inverse $\chi_M T$ with respect to temperature is shown in Figure 9 for complex **2d**. The ground term of free Sm(III) ion is $^6H_{5/2}$ and it splits into six states by spin-orbit coupling at room temperature. The ground state $^6H_{5/2}$ is not completely separated from the excited ones (about 700 cm^{-1} from the ground state to the first excited state). Hence, both the possible thermal population and the crystal field effect of the high states should be evaluated for the Sm(III) complex.^{16,18} From the Figure 9, it can be seen, the $\chi_M T$ value is equal to 0.78 $\text{emu mol}^{-1}\text{K}$ at 300K, which is close to expected 0.84 $\text{emu mol}^{-1}\text{K}$ for two magnetically isolated Sm(III) ion ($S = 5/2$, $L = 5/2$, $^6H_{5/2}$, $g = 2/7$).^{16,18} When the temperature was cooled to 2K, the $\chi_M T$ decreases monotonically and rapidly to a value of 0.14 $\text{emu mol}^{-1}\text{K}$. The thermal variation of $\chi_M T$ is practically linear over the whole temperature range. The linear thermal variation of $\chi_M T$ is reported for Sm(III) complexes in the literature.¹⁹ This behavior indicates that an antiferromagnetic interaction possibly exists between Sm(III) pairs at lower temperature, although it is very weak.

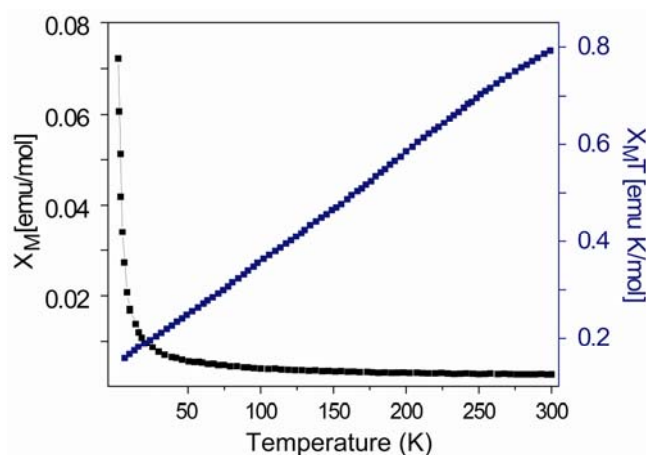


Figure 9. Plots of the temperature dependence of $\chi_M T$ and χ_M for **2d**.

The magnetic characteristic of complex **2e** is different from that of **2d**. The $\chi_M T$ value of 23.48 $\text{emu mol}^{-1}\text{K}$ observed at room temperature is close to the value of 23.64 $\text{emu mol}^{-1}\text{K}$ expected for two noninteracting Tb(III) ions (7F_6 , $S = 3$, $L = 3$, $g = 3/2$).^{16,20} Upon cooling the system, $\chi_M T$ continuously decreases over the whole temperature range and reaches 10.34 $\text{emu mol}^{-1}\text{K}$ at 2 K comparable with the results reported previously.²⁰ The plot of inverse χ_M with temperature shows a straight line and also follows Curie–Weiss law with a Weiss constant, $\theta = -25.5$ K. However, negative value of θ and the trends of the $\chi_M T$ values cannot clearly corroborate the antiferromagnetic coupling between two neighboring Tb(III) ions.

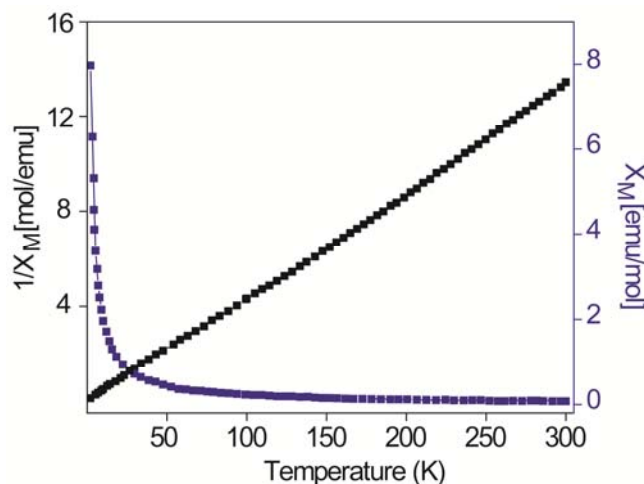


Figure 10. Plots of the temperature dependence of χ_M and $1/\chi_M$ for compound **2e**.

Conclusions

In summary, we have successfully synthesized nine coordination polymers with BNA and 3,5-PDC ligands and different metal ions. Solvent selection and reaction conditions play an important role in the crystallization process to reveal new structures (**1a** and **1b**) with BNA ligand, which represent either pseudo-polymorph or supramolecular isomer of the known ones. They exhibit distinct Br \cdots O halogen bonding interactions, which may provide an additional reason for the diversification of the coordination modes with this ligand. The five new coordination complexes of 3,5-PDC with d-metal ions (**2a**, **2b** and **2c**) and f-metal ions (**2d** and **2e**) are characterized by single crystal X-ray diffraction analysis. The small rigid ligand 3,5-H₂PDC is achiral in nature. Nevertheless, it yielded three chiral coordination-polymeric structures (**2b**, **2c** and **2e**). The four lanthanoid MOFs (**2d**, **2e**, **2f** and **2g**) are essentially isostructural to each other (**2d**, **2f** and **2g** being isomorphous). Networking diversity in the analyzed series of coordination complexes is due primarily to the coordination environment of the metal ions. In the case of lanthanoid MOFs (**2d-2g**) pyridyl-N of 3,5-PDC does not take part in metal-coordination. Nevertheless, the larger size and coordination number (as well as the unique optical properties) of the oxophilic lanthanoid reagents (as compared to the d-metals) make them more attractive nodes for targeted crystal engineering of 3D framework solids. The magnetic study of the complex **2a** reveals weak antiferromagnetic coupling between the metal centers through carboxylate bridges. In the **2d** and **2e** there may be some antiferromagnetic interaction between the proximate metal centers but the degree of interaction is difficult to determine. The above discussed materials provide an important expansion of the continuously increasing database of metal-organic coordination networks and the crystal engineering tools that contribute to their formation. The 3D MOF materials with Ln-ion connectors are of further

interest in the context of guest storage and exchange within the intra-lattice channels and formation of metallogels. Studies along these directions are currently underway.

Acknowledgements

This research was supported by the Israel Science Foundation (Grant No. 108/12).

* Electronic supplementary information (ESI) available: X-ray crystallographic details in CIF format. CCDC 981479-981485 (**1a-2e**), 979166 (**2f**) and 979167 (**2g**). For crystallographic data in CIF or other electronic format see DOI: 10.1039/xxxxxxxxxx.

References:

- (a) R. J. Kuppler, D. J. Timmons, Q.-R. Fang, J.-R. Li, T. A. Makal, M. D. Young, D. Yuan, D. Zhao, W. Zhuang and H.-C. Zhou, *Coord. Chem. Rev.*, 2009, **253**, 3042; (b) M. Kurmoo, *Chem. Soc. Rev.*, 2009, **38**, 1353; (c) J. Y. Lee, O. K. Farha, J. Roberts, K. A. Scheidt, S. B. T. Nguyen and J. T. Hupp, *Chem. Soc. Rev.*, 2009, **38**, 1450; (d) E. Coronado and G. M. Espallargas, *Chem. Soc. Rev.*, 2013, **42**, 1525; (e) J.-R. Li, J. Sculley and H.-C. Zhou, *Chem. Rev.*, 2012, **112**, 869; (f) R. B. Getman, Y.-S. Bae, C. E. Wilmer and R. Q. Snurr, *Chem. Rev.*, 2012, **112**, 703; (g) K. Sumida, D. L. Rogow, J. A. Mason, T. M. McDonald, E. D. Bloch, Z. R. Herm, T.-H. Bae and J. R. Long, *Chem. Rev.*, 2012, **112**, 724; (h) S. Chaemchuen, N. A. Kabir, K. Zhou and F. Verpoort, *Chem. Soc. Rev.*, 2013, **42**, 9304; (i) H. Furukawa, K. E. Cordova, M. O'Keeffe and O. M. Yaghi, *Science*, 2013, **341**, 974; (j) L. J. Murray, M. Dincă and J. R. Long, *Chem. Soc. Rev.*, 2009, **38**, 1294; (k) F. A. A. Paz, J. Klinowski, S. M. F. Vilela, J. P. C. Tomé, J. A. S. Cavaleiro and J. Rocha, *Chem. Soc. Rev.*, 2012, **41**, 1088; (l) D. Zacher, O. Shekhah, C. Wöll and R. A. Fischer, *Chem. Soc. Rev.*, 2009, **38**, 1418.
- (a) R. Patra, H. M. Titi and I. Goldberg, *CrystEngComm*, 2013, **15**, 2853; (b) R. Patra, H. M. Titi and I. Goldberg, *CrystEngComm*, 2013, **15**, 2863; (c) R. Patra, H. M. Titi and I. Goldberg, *New J. Chem.*, 2013, **37**, 1494; (d) R. Patra, H. M. Titi and I. Goldberg, *CrystEngComm*, 2013, **15**, 7257; (e) A. Karmakar and I. Goldberg, *CrystEngComm*, 2011, **13**, 350; (f) A. Karmakar and I. Goldberg, *CrystEngComm*, 2011, **13**, 339; (g) A. Karmakar, H. M. Titi, and I. Goldberg, *Cryst. Growth Des.*, 2011, **11**, 2621.
- (a) S. Yi-Shan, Y. Bing and C. Zhen-Xia, *J. Solid State Chem.*, 2004, **177**, 3805; (b) C-P. Li, J-M. Wu and M. Du *Chem. Eur. J.*, 2012, **18**, 12437; (c) C-P. Li, J. Chen, P-W. Liu and M. Du, *CrystEngComm*, 2013, **15**, 9713; (d) J. Y. Lu and L. Chen, *Inorg. Chem. Commun.*, 2004, **7**, 350.
- (a) A. Mallick, S. Saha, P. Pachfule, S. Roy and R. Banerjee, *J. Mater. Chem.*, 2010, **20**, 9073; (b) X.-P. Zhang, G. Yang and S. W. Ng, *Acta Cryst.*, 2006, **E62**, m791; (c) J.-c. Yao, J.-b. Guo, J.-g. Wang, Y.-f. Wang, L. Zhang and C.-p. Fan, *Inorg. Chem. Commun.*, 2010, **13**, 1178; (d) T. Furuta, I. Kanoya, H. Sakai and M. Hosoe, *Polymers*, 2011, **3**, 2133.

5. X. Wang, Q-G. Zhai, S-N. Li, Y-C. Jiang and M-C. Hu, *Cryst. Growth Des.*, 2014, **14**, 177.
6. G. Nandi, H. M. Titi, R. Thakuria and I. Goldberg, Unpublished work.
7. G. A. Bain and J. F. Berry, *J. Chem. Educ.*, 2008, **85**, 532.
8. A. Altomare, G. Cascarano, C. Giacovazzo, A. Guagliardi, M. C. Burla, G. Polidori and M. Camalli, *J. Appl. Crystallogr.*, 1994, **27**, 435.
9. G. M. Sheldrick, *Acta Crystallogr.*, 2008, **A64**, 435.
10. J. C. Antonio, M. E. López-Viseras, A. Salinas-Castillo, D. Fairen-Jimenez, E. Colacio, J. Canod and A. Rodríguez-Diéguez *CrystEngComm.*, 2012, **14**, 6390.
11. V. A. Blatov, IUCr Comput. Comm. Newsl. 2006, 7, 4–38; <http://www.topos.ssu.samara.ru>
12. S. S. Batsanov, *Inorg. Mater.*, 2001, **37**, 871.
13. (a) B. Moulton and M. J. Zaworotko, *Chem. Rev.*, 2001, **101**, 1629; (b) J.-P. Zhang, X.-C. Huang and X.-M. Chen, *Chem. Soc. Rev.*, 2009, **38**, 2385; (c) G. Mehlana, S. A. Bourne, G. Ramon and L. Öhrström, *Cryst. Growth Des.*, 2013, **13**, 633.
14. (a) P. Kanoo, K. L. Gurunatha and T. K. Maji, *Cryst. Growth Des.*, 2009, **9**, 4147; (b) M. J. Katz, T. Ramnial, H.-Z. Yu and D. B. Leznoff, *J. Am. Chem. Soc.*, 2008, **130**, 10662; (c) F. Dai, H. He and D. Sun, *Inorg. Chem.*, 2009, **48**, 4613.
15. (a) O. Delgado Friedrichs, M. O'Keeffe and O. M. Yaghi, *Acta Cryst.* (2003). **A59**, 22-27; (b) O. Delgado-Friedrichs, Systre and 3dt, programs are free available on line: <http://gavrog.org/>.
16. (a) R. L. Carlin, Magnetochemistry, *Springer-Verlag, Berlin, Heidelberg*, 1986; (b) O. Kahn, Molecular Magnetism, *VCH, Berlin*, 1993, p. 380.
17. (a) J. P. Zhao, B. W. Hu, Q. Yang, X. F. Zhang, T. L. Hu and X. H. Bu, *Dalton Trans.*, 2010, **39**, 56; (b) M. Y. Zhang, W. J. Shan and Z. B. Han, *CrystEngComm.*, 2012, **14**, 1568.
18. H. H. Song, Y. J. Li, Y. Song, Z. G. Han and F. Yang, *J. Solid State Chem.*, 2008, **181**, 1017.
19. (a) A. Q. Wu, F. K. Zheng, W. T. Chen, L. Z. Cai, G. C. Guo, J. S. Huang, Z. C. Dong and Y. Takano, *Inorg. Chem.*, 2004, **43**, 4839. (b) R. Martínez-Máñez and F. Sancenón, *Chem. Rev.*, 2003, **103**, 4419; (c) C. Seward, N. X. Hu and S. Wang, *J. Chem. Soc., Dalton Trans.*, 2001, 134. (d) X. Feng, X. -L. Ling, L. Liu, H. -L. Song, L. Y. Wang, S. W. Ng and B. Y. Su, *Dalton Trans.*, 2013, **42**, 10292.
20. (a) T. H. Zhou, F. Y. Yi, P. X. Li and J. G. Mao, *Inorg. Chem.*, 2010, **49**, 905; (b) X. D. Guo, G. S. Zhu, Z. Y. Li, F. X. Sun, Z. H. Yang and S. L. Qiu, *Chem. Commun.*, 2006, 3172; (c) T. Kajiwara, M. Hasegawa, A. Ishii, K. Katagiri, M. Baatar, S. Takaishi, N. Iki and M. Yamashita, *Eur. J. Inorg. Chem.*, 2008, 5565; (d) J. P. Costes, J. M. C. Juan, F. Dahan and F. Nicodème, *J. Chem. Soc., Dalton Trans.*, 2003, 1272.

Graphical abstract

Nine new metallo-organic coordination polymers of 5-substituted nicotinic acid (with either –Br, HBNA, or –COOH, 3,5-H₂PDC) with various d- and f-transition metal ions have been synthesized and structurally characterized. Networking diversity observed in these 2D and 3D coordination assemblies with this ligand is discussed.

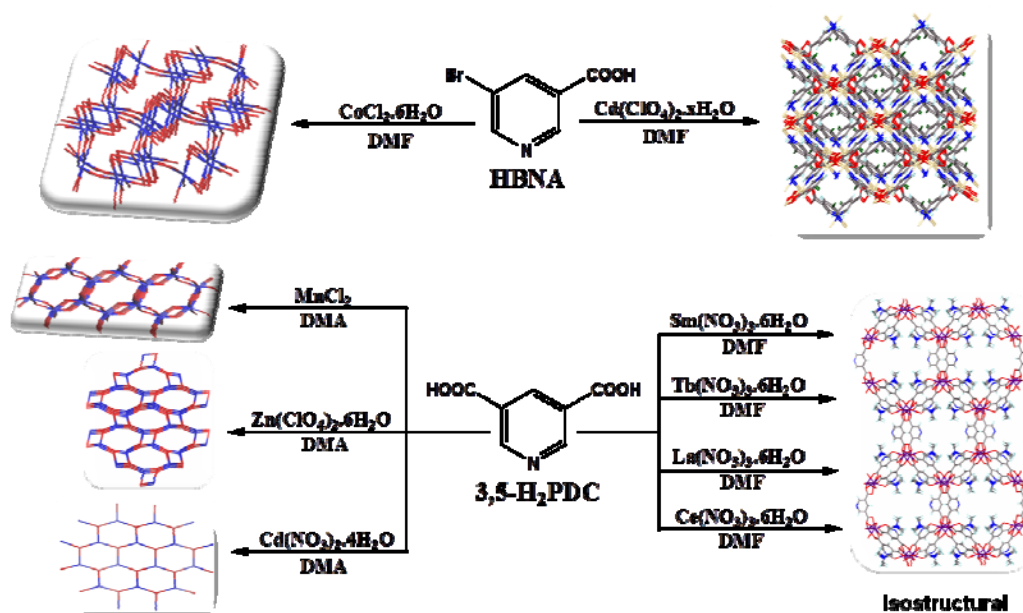


Table 1 Crystal data and Structure Refinement Summary for complexes 1a-b, 2a-g

	1a ^a	1b	2a ^a	2b	2c	2d ^a	2e ^a	2f ^a	2g ^a
Chemical formula	C ₂₄ H ₁₄ Br ₄ Co ₂ N ₄ O ₉	C ₁₂ H ₆ Br ₂ CdN ₂ O ₄	C ₃₁ H ₃₀ Mn ₃ N ₆ O ₁₅	C ₁₁ H ₁₂ N ₂ O ₅ Zn, C ₄ H ₉ NO	C ₁₅ H ₂₁ CdN ₃ O ₆	C ₂₇ H ₂₃ N ₅ O ₁₄ Sm ₂	C ₂₇ H ₂₃ N ₅ O ₁₄ Tb ₂	C ₂₇ H ₂₃ La ₂ N ₅ O ₁₄	C ₂₇ H ₂₃ Ce ₂ N ₅ O ₁₄
Formula weight	939.85	514.41	891.43	404.72	451.75	942.20	959.34	919.32	921.74
Crystal system	Monoclinic	Monoclinic	Monoclinic	Orthorhombic	Monoclinic	Orthorhombic	Orthorhombic	Orthorhombic	Orthorhombic
Space group	<i>P2₁/n</i>	<i>C2/c</i>	<i>P2₁/n</i>	<i>P2₁2₁2₁</i>	<i>P2₁</i>	<i>Pnma</i>	<i>P2₁2₁2₁</i>	<i>Pnma</i>	<i>Pnma</i>
T/K	110	110	110	110	110	110	110	110	110
a/Å	14.2109(5)	12.0504(3)	13.2579(5)	10.8285(4)	9.2879(3)	8.02340(10)	8.5085(4)	8.1241(3)	8.1162(4)
b/Å	17.6868(6)	9.9837(2)	11.4380(3)	11.1933(4)	11.9733(3)	30.2439(5)	16.0156(8)	30.3843(10)	30.2842(14)
c/Å	14.2110(5)	24.8139(5)	28.7450(10)	14.7990(6)	16.3513(5)	15.3280(2)	27.9393(14)	15.6616(5)	15.6709(7)
α/°	90	90	90	90	90	90	90	90	90
β/°	118.306(2)	101.2980(10)	99.887(2)	90	101.7090(16)	90	90	90	90
γ/°	90	90	90	90	90	90	90	90	90
Z	4	8	4	4	4	4	4	4	4
V/Å ³	3144.77(19)	2927.45(11)	4294.3(2)	1793.74(12)	1780.54(9)	3719.48(9)	3807.3(3)	3866.0(2)	3851.8(3)
D _{calc} /g cm ⁻³	1.985	2.334	1.379	1.499	1.685	1.683	1.674	1.579	1.589
μ/mm ⁻¹	6.191	6.966	0.935	1.405	1.262	3.192	3.748	2.243	2.397
Reflns collected	24928	12286	29739	17170	14664	19671	18953	24239	15168
Unique reflns	4638	2730	6555	4186	6186	4076	6494	3262	2869
R1[I > 2(I)]	0.0373	0.0233	0.0668	0.0283	0.0328	0.0294	0.0418	0.0434	0.0401
wR2 (all)	0.1034	0.0457	0.1727	0.0639	0.0653	0.0758	0.1008	0.1085	0.1004
Goodness-of-fit	1.089	1.084	1.043	1.042	1.061	1.000	1.060	1.080	1.087

^a Excluding an additional DMF/DMA intra-lattice non-coordinated and severely disordered solvent. The *R*-factors refer to crystallographic least-squares refinements based on PLATON-squeezed data.

Graphical abstract

New coordination polymers of 5-substituted nicotinic acid with metal ions have been characterized, revealing diversely interlinked 2D and 3D architectures.

